Indonesian Geotechnical Journal, August 2026, Vol 5 (2). Page 75-88
DOI: https://doi.org/10.56144/igj.v5i2.162
EISSN: 2829-7520
https://indonesian-geotechnical-journal.org/index.php/JGI/issue/archive

Derivation of Elastic Parameters from Integrated Seismic Refraction Tomography and Multichannel Analysis of Surface Waves (MASW) for Geotechnical Site Characterization at APT Pranoto Airport, Samarinda, East Kalimantan

Mita Diniyarti[1,3*], Piter Lepong[2,3], Wahidah[2,3], Supriyanto[1,3], Zetsaona Sihotang[2]
[1] Department of Physics, Faculty of Mathematics and Natural Sciences, Mulawarman University, Samarinda, Indonesia, 75119
[2] Department of Geophysics, Faculty of Mathematics and Natural Sciences, Mulawarman University, Samarinda, Indonesia, 75119
[3]Geophysics Laboratory, Faculty of Mathematics and Natural Sciences, Mulawarman University, Samarinda, Indonesia, 75119
*Correspondence: pit.lepong@gmail.com

SUBMITTED 25 May 2026 **REVISED** 6 August 2026 **ACCEPTED** 18 August 2026

ABSTRACT APT Pranoto Samarinda Airport is a transportation infrastructure facility that has experienced subsidence in the taxiway area, indicating potential issues related to subsurface conditions. This study aims to determine the distribution of dynamic elastic parameters, estimate the approximate groundwater table position, and evaluate the brittleness of subsurface materials via seismic refraction tomography (SRT) and multichannel analysis of surface waves (MASW). The derived parameters include Young's modulus, bulk modulus, shear modulus, and Poisson's ratio. The brittleness index was used to evaluate material brittleness, while the V_p/V_s ratio was used to estimate the approximate groundwater table position. The interpreted dynamic elastic parameters were qualitatively compared with lithological information and standard penetration test (SPT) data obtained from nearby soil borings to support the interpretation of subsurface conditions. The results indicate that shallow layers exhibit relatively lower Young's, shear, and bulk modulus values than deeper layers. In contrast, deeper layers exhibit higher elastic parameter values, while the brittleness index indicates a transition from relatively ductile shallow materials to more brittle materials at greater depths. The V_p/V_s distribution suggests an approximate groundwater table at depths of 2.5–3 m. Relatively high Poisson's ratio values in some zones may reflect pore-fluid influence on the elastic response of the subsurface materials. However, it should be noted that Poisson's ratio alone is insufficient to establish groundwater saturation. At depths greater than 15 m, higher elastic parameter values generally correspond to higher nearby SPT values. However, these dynamic elastic parameters should not be interpreted as direct measures of geotechnical soil stiffness. These subsurface characteristics may help explain the deformation susceptibility of the taxiway area; however, the specific cause and depth interval responsible for the observed subsidence cannot be determined from the present data alone.

KEYWORDS Elastic parameters; Seismic refraction tomography; Multichannel analysis of surface waves

1 INTRODUCTION

APT. Pranoto Airport is a key transportation infrastructure facility that supports mobility and economic activity in East Kalimantan. However, repeated subsidence has occurred in the taxiway area, indicating potential geotechnical problems within the subsurface. This situation highlights the need for further investigation. In this study, seismic refraction tomography (SRT) and multichannel analysis of surface waves (MASW) were employed to obtain dynamic mechanical characteristics of subsurface materials.

In geotechnical studies, the seismic refraction tomography (SRT) and multichannel analysis of surface waves (MASW) exhibit different sensitivities to subsurface conditions. The SRT method utilizes compressional wave velocity (V_p) to characterize subsurface variations, including differences in lithology and material properties (Fadhli et al., 2022). Meanwhile, MASW uses shear-wave velocity (V_s) to characterize the relative small-strain dynamic stiffness of subsurface materials (Olafsdottir et al., 2020). The integration of these two methods allows for a more comprehensive determination of elastic parameters such as Young's modulus, shear modulus, bulk modulus, and Poisson's ratio, and helps identify weak zones that could potentially cause subsidence in the taxiway area.

Several previous studies have utilized geophysical methods to characterize subsurface conditions and elastic parameters. Ketelhodt et al. (2017) demonstrated that the integration of compression and shear waves can yield elastic parameters in the form of two-dimensional cross-sections. Rizqulloh et al. (2021) also integrated seismic refraction tomography and multichannel analysis of surface waves to analyse the distribution of elastic parameters and brittleness indices, supported by nearby soil penetration test data for subsurface interpretation. However, this research still has limitations in presenting elastic parameters in an integrated and comprehensive manner, particularly in combining elastic parameter analysis with the identification of subsurface saturation conditions, including the determination of the groundwater table.

This study aims to determine the distribution of dynamic elastic parameters of subsurface materials, estimate the groundwater-table position, and evaluate the dynamic elastic characteristics and brittleness of the subsurface. The interpreted seismic results were qualitatively compared with lithological information and standard penetration test (SPT) data from nearby soil borings.

2 METHODS

This study is a quantitative study using a shallow geophysical approach that integrates seismic refraction tomography and multichannel analysis of surface waves (MASW) to determine the elastic parameters of subsurface materials in the taxiway area of APT. Pranoto Airport in Samarinda. The integration of these two methods was chosen because it can provide information on primary wave velocity (V_p) and shear wave velocity (V_s), allowing for a comprehensive calculation of elastic parameters of subsurface materials (Rizqulloh et al., 2021). The study was conducted in the taxiway area of APT Pranoto Airport in Samarinda, East Kalimantan, which had previously experienced subsidence. The study location and measurement paths are shown in Figure 1.

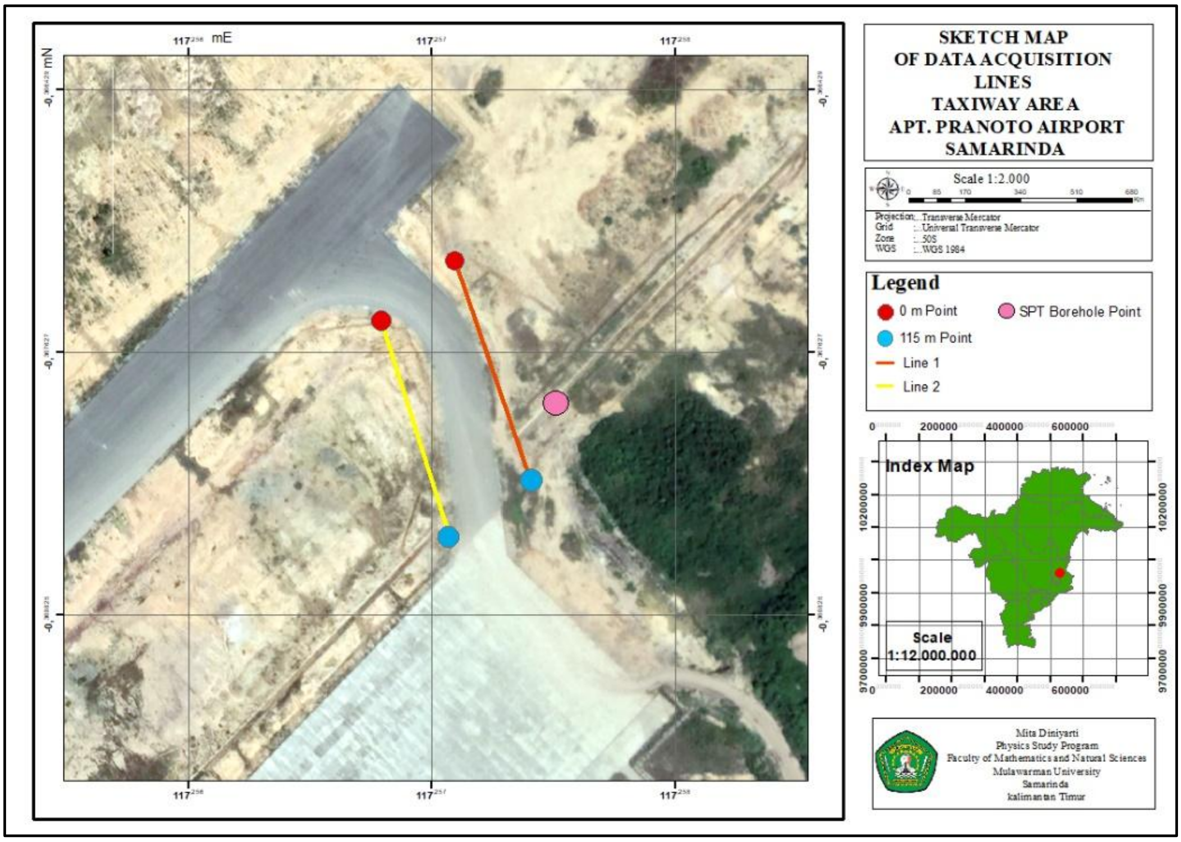

Figure 1. Location of the survey line in the taxiway area at APT. Pranoto Airport.

This study uses secondary data in the form of primary wave velocity (V_p) distributions, secondary wave velocity (V_s) distributions, and standard penetration test (SPT) data. The primary wave velocity (V_p) data were obtained from the digitization of cross-sectional data processed by Fatimatuzzahra (2024) using the seismic refraction tomography method, while secondary wave velocity (V_s) data were obtained from the digitization of cross-sections processed by Simbolon (2024) using the multichannel analysis of surface waves (MASW) method. Secondary data were chosen because the results of previous studies already represent the subsurface conditions of the study area and are considered adequate for analysing elastic parameters.

The V_p data obtained from the seismic refraction tomography method are used to characterize the subsurface distribution of compressional wave velocity. The seismic refraction tomography method utilizes the analysis of the first arrival time (first break) of seismic waves to generate a two-dimensional distribution of primary wave velocity. This method was selected because it provides adequate subsurface resolution for characterizing lateral and vertical variations in compressional-wave velocity associated with differences in lithology and subsurface material properties (Abdullah et al., 2019; Alamsyah et al., 2024). Meanwhile, V_s data from the MASW method are used to characterize the subsurface shear wave velocity distribution based on Rayleigh wave dispersion analysis. The MASW method was chosen because it is effective in deriving shear-wave velocity (V_s) profiles within the investigated shallow subsurface interval, which extends to approximately 23 m in this study. These profiles are used to characterize relative variations in the small-strain dynamic stiffness of the subsurface materials (Zawawi et al., 2023; Hamdan et al., 2025).

The data processing stage involved digitizing the cross-sections of the primary (V_p) and secondary (V_s) wave velocity distributions from a previous study to obtain velocity values at each depth and along each path. This data is used to calculate and visualize elastic parameters, namely shear modulus (G), Young's modulus (E), bulk modulus (K), Poisson's ratio (ν), the V_p/V_s ratio, and the brittleness index (Brittleness Index/BI). The calculation results were then visualized in the form of two-dimensional (2D) cross-sections to illustrate the lateral and vertical distribution of subsurface mechanical properties.

Bulk density was estimated from P-wave velocity using Gardner's equation,

$$\rho = aV_p^{\frac{1}{4}} \tag{1}$$

ρ is the density (kg/m³), V_p is the primary wave velocity (m/s), and a is an empirical constant of 0.31. It should be noted that the equation was originally derived for saturated clastic sedimentary rocks. Its accuracy for the unconsolidated soil layers was not independently verified; therefore, the density and the derived G, E, and K values, particularly in shallow layers, should not be used directly for design. These moduli are consequently interpreted as apparent small-strain dynamic parameters rather than modulus at the typical geotechnical design strain level (Gardner et al., 1974):

The Poisson's ratio is calculated using the relationship between the primary and secondary wave velocities as follows (Lógó et al., 2022):

$$\nu = \frac{1}{2}\left(1 - \frac{1}{\left(\frac{V_p^2}{V_s^2}\right) - 1}\right) \tag{2}$$

Where ν denotes the Poisson's ratio; V_p is the primary wave velocity (m/s), while V_s is the secondary wave velocity (m/s).

The shear modulus is calculated using the equation by Sarkar et al. (2021):

$$G = \rho V_s^2 \tag{3}$$

where G is the shear modulus (MPa), ρ is the density calculated from equation 1 (kg/m³), and V_s is the secondary wave velocity (m/s).

Young's modulus is also calculated using the equation by Sarkar et al. (2021):

$$E = (\rho V_s^2) \left(\frac{3V_p^2 - 4V_s^2}{V_p^2 - V_s^2} \right) \tag{4}$$

Where E is Young's modulus (MPa), ρ is density calculated from equation 1 (kg/m³), V_p is the primary wave velocity (m/s), and V_s is the secondary wave velocity (m/s).

The bulk modulus is calculated using the equation by Omovie et al. (2020):

$$K = \rho \left(V_p^2 - \frac{4}{3} V_s^2 \right) \tag{5}$$

Where K represents the bulk modulus (MPa), ρ represents density (kg/m³), V_p is the primary wave velocity (m/s), and V_s is the secondary wave velocity (m/s).

The brittleness index (BI) was calculated based on the normalized Young's modulus and Poisson's ratio using the equation proposed by Mews et al. (2019):

$$BI = \frac{E_{\text{norm}} + (1 - \nu_{\text{norm}})}{2} \tag{6}$$

Where,

$$E_{\text{norm}} = \frac{E - E_{\text{min}}}{E_{\text{max}} - E_{\text{min}}}, \nu_{\text{norm}} = \frac{\nu - \nu_{\text{min}}}{\nu_{\text{max}} - \nu_{\text{min}}} \tag{7}$$

E is Young's modulus (MPa), E_{min} and E_{max} are the minimum and maximum values of Young's modulus from the entire dataset, respectively, ν is Poisson's ratio, ν_{min} and ν_{max} are the minimum and maximum values of Poisson's ratio from the entire dataset, respectively, while E_{norm} and ν_{norm} are the normalized values of Young's modulus and Poisson's ratio. The brittleness index values are classified into four levels as shown in Table 1.

Table 1. Classification of Brittleness Index (Altamar et al., 2014)

Value Range	Description
< 0.16	Ductile
0.16–0.32	Less ductile
0.32–0.48	Less brittle
> 0.48	Brittle

The analysis was conducted descriptively based on variations in parameter values with depth. Interpretation of subsurface conditions was performed by comparing elastic modulus values, the V_p/V_s ratio, and SPT data. Layers with high elastic modulus and high SPT values were interpreted as more compact and rigid materials, while layers with high Poisson's ratio and large V_p/V_s ratios were interpreted as materials that tend to be water-saturated and softer in nature.

3 RESULTS

The distributions of shear modulus, Young's modulus, bulk modulus, Poisson's ratio, brittleness index, and V_p/V_s ratio are shown in Figures 2–7. In general, the elastic parameters show an increase in value with depth, while Poisson's ratio and the V_p/V_s ratio tend to be high in shallow layers and decrease at greater depths. The brittleness index cross-section shows variations in material brittleness ranging from less ductile to brittle. The distribution of these parameters reflects variations in subsurface mechanical characteristics in the study area.

3.1 Shear Modulus

Figure 2 shows the interpreted shear modulus along line 1 and 2. The shear modulus profile shows relative variations in the small-strain dynamic resistance of the subsurface materials to shear deformation. Within expectation, higher values generally occur at greater depths and indicate a stiffer dynamic response, whereas lower values occur in shallower intervals. Localized reductions in shear modulus represent zones of comparatively lower dynamic stiffness but cannot independently confirm the presence of geotechnical weak zones.

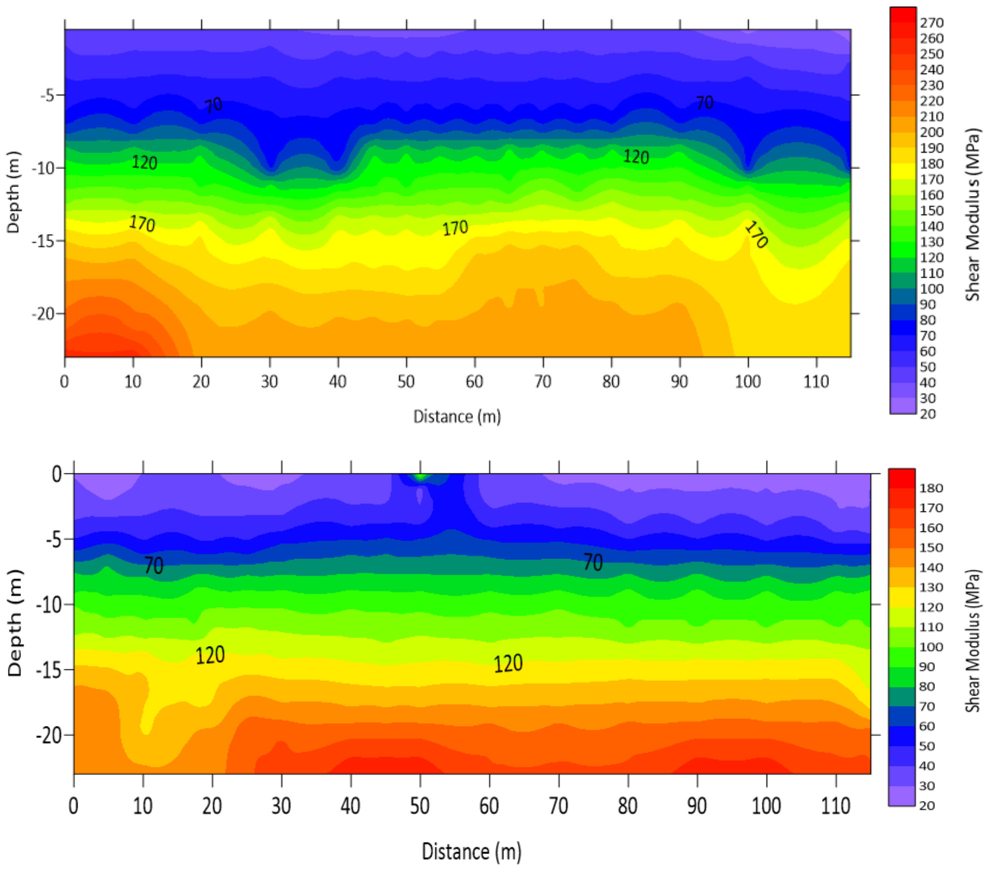

Figure 2. Cross-sections showing the shear modulus for line 1 (top) and line 2 (bottom)

3.2 Young's Modulus

Figure 3 shows the interpreted Young's modulus along line 1 and 2. The Young's modulus profile illustrates lateral and vertical variations in the small-strain dynamic stiffness of the subsurface materials. Since the Young's modulus were derived from seismic-wave velocities and estimated density, they represent dynamic rather than static Young's modulus. Hence the very high Young's modulus interpreted, for example, 300 MPa at depth of 10 m for line 1 and 2. Therefore, these results should be interpreted primarily as relative variations in dynamic stiffness and cannot be used to determine the likelihood of subsidence under operational loading conditions.

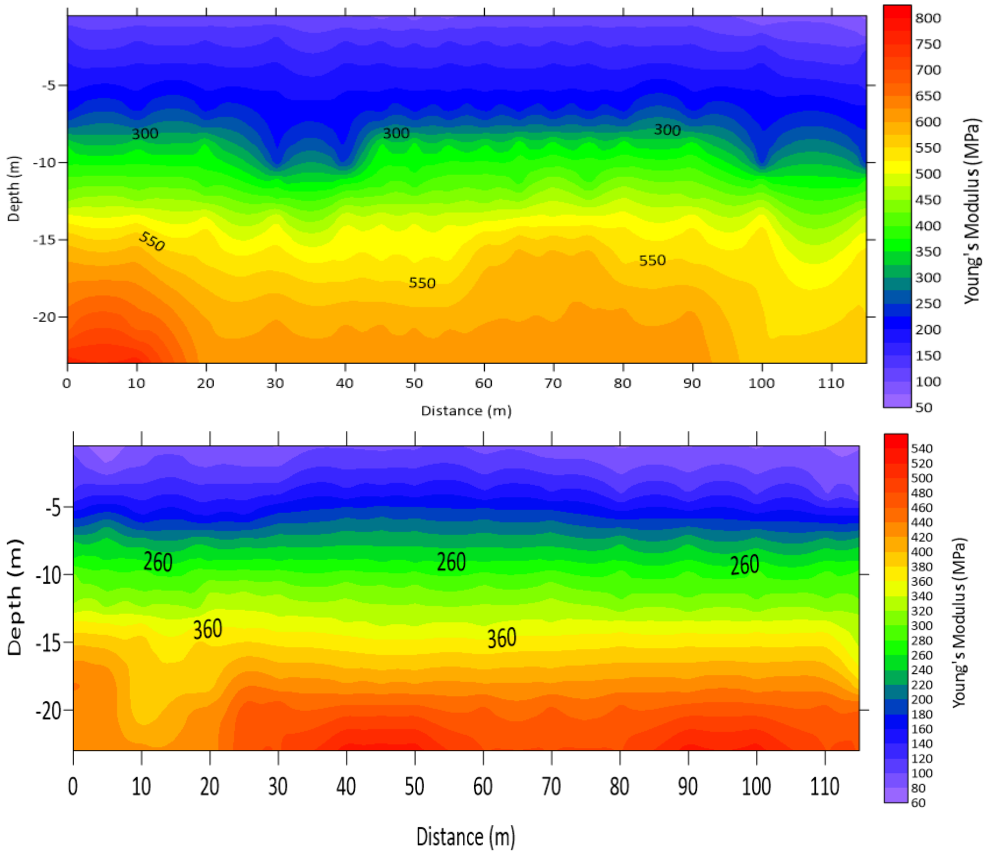

Figure 3. Cross-sections showing Young's modulus for line 1 (top) and line 2 (bottom)

3.3 Bulk Modulus

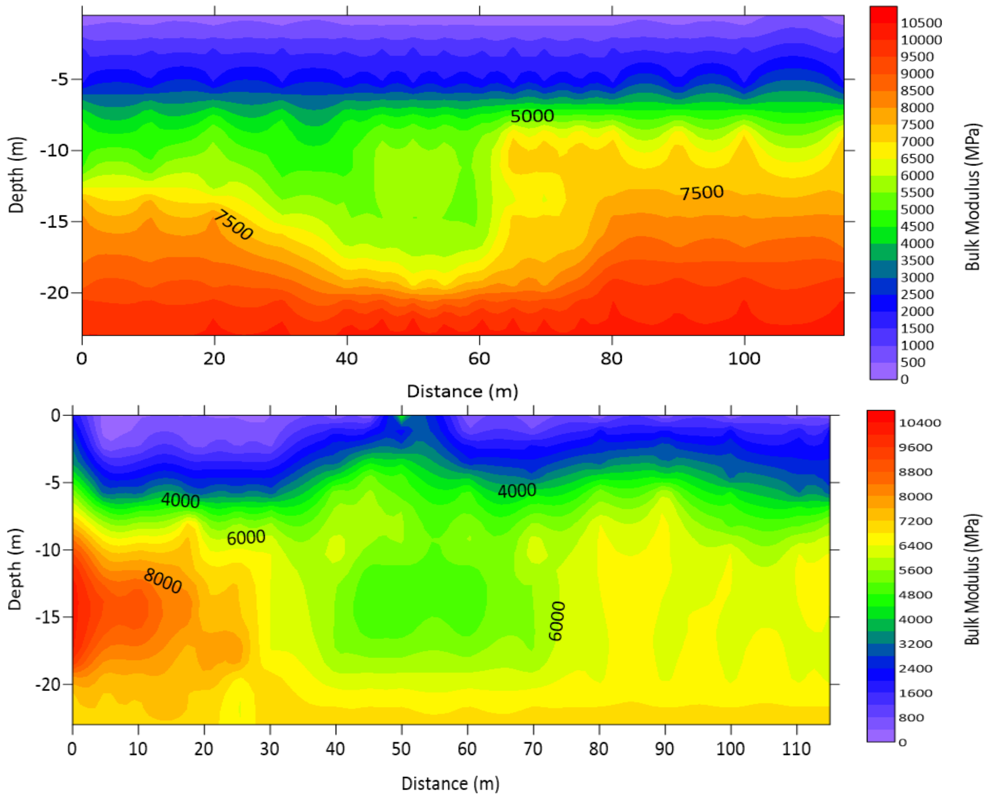

Figure 4. Cross-sections showing the bulk modulus for line 1 (top) and line 2 (bottom)

Figure 4 shows the interpreted bulk modulus along line 1 and 2. The bulk modulus cross-section shows lateral and vertical variations in the small-strain dynamic resistance to volumetric deformation. Although some low-modulus zones coincide with high V_p/V_s and Poisson's ratio values that may reflect pore-fluid effects, the available data are insufficient to link them directly to the observed subsidence. It should also be noted that the obtained bulk modulus is extremely high, typically between 1-50 MPa for clays, and 300 MPa for gravel. However, the interpreted bulk modulus is in the range of 1000-10000 MPa.

3.4 Poisson's Ratio

Figure 5 shows the interpreted Poisson's ratio along line 1 and 2. The Poisson's ratio profiles show variations in the elastic response of the subsurface materials. Line 2 generally exhibits higher Poisson's ratio values than Line 1, with most areas approaching 0.5. These relatively high values indicate lower volumetric compressibility and may reflect the influence of pore fluids on the elastic behavior of the subsurface materials. It should be noted that Poisson's ratio for soil is typically in the range of 0.3-0.4, with the exception of undrained saturated clay. Further investigation is required whether the Poisson's ratios obtained from SRT or MASW are representative to the soil's actual behaviour.

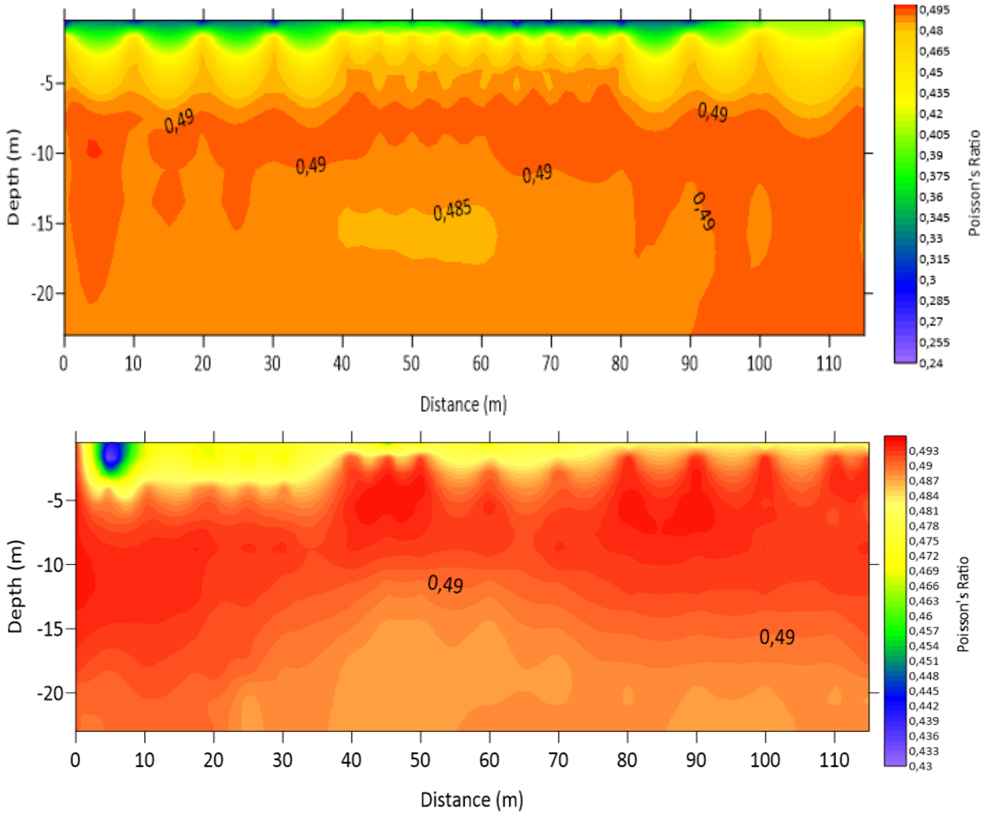

Figure 5. Cross-sections showing Poisson's ratio for line 1 (top) and line 2 (bottom)

3.5 Brittleness Index

Figure 6 shows the interpreted Brittleness Index (BI) along line 1 and 2. The BI profiles show variations in the mechanical behavior of subsurface materials. In Line 1, relatively higher BI values of around 3 were interpreted in the very shallow layer (approximately 0–1.5 m), followed by lower values of around 0.04 to 0.16 at depths of 1.5–10 m. This variation may reflect differences in near-surface mechanical conditions, where the shallowest layer may exhibit greater brittleness due to reduced confining pressure and possible compaction or weathering effects, while the underlying layer shows a more ductile response. Deeper zones with increasing BI values indicate stronger brittle characteristics. However, BI variations should be interpreted together with other elastic parameters for a more comprehensive evaluation of subsurface mechanical properties.

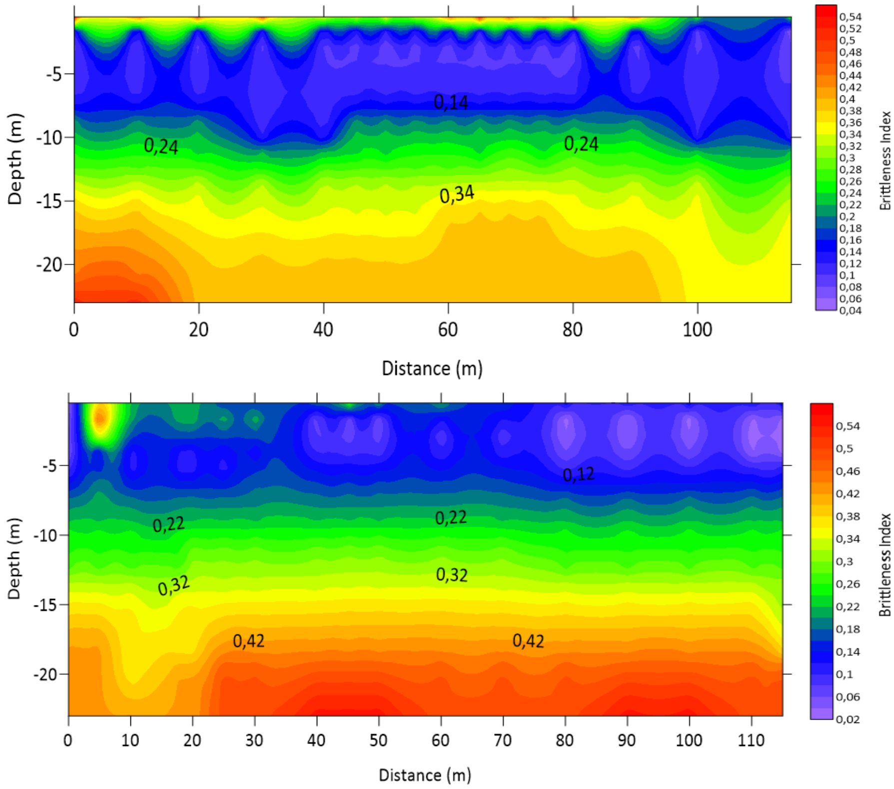

Figure 6. Cross-sections showing the brittleness index for line 1 (top) and line 2 (bottom)

3.6 V_p/V_s Ratio

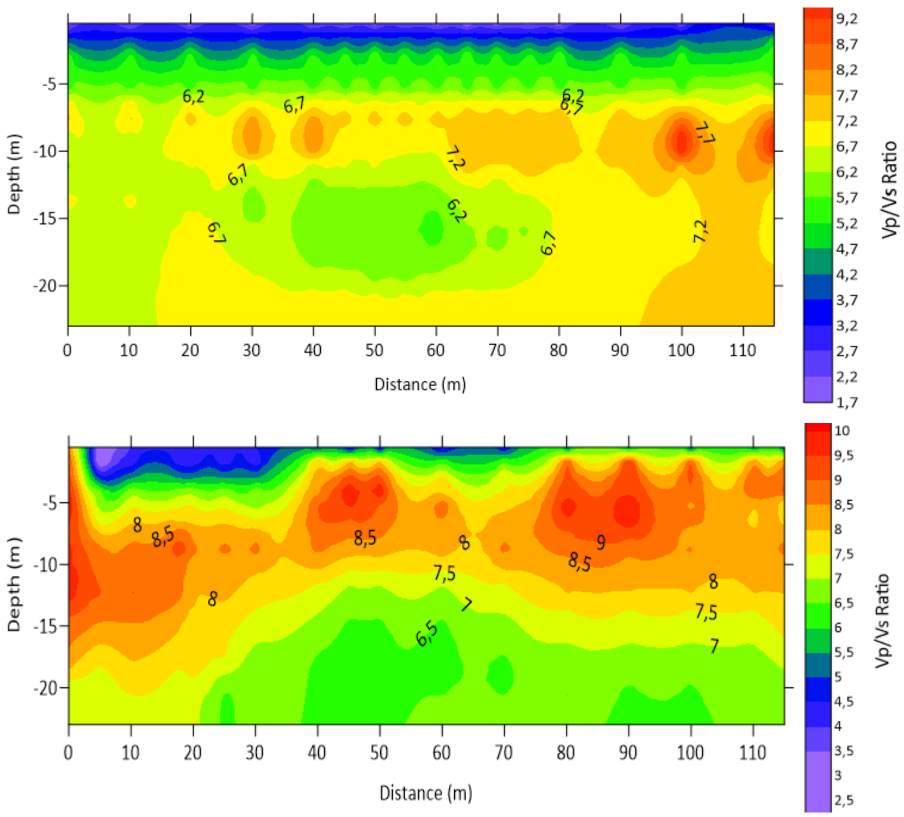

Figure 7. Cross-sections showing the V_p/V_s ratio for line 1 (top) and line 2 (bottom)

Figure 7 shows the calculated V_p/V_s along line 1 and 2. The V_p/V_s ratio varies with depth and reflects changes in subsurface material properties. Lower values are generally associated with unsaturated to partially saturated materials, whereas higher values may indicate pore-fluid influence or greater saturation. The profile has to be interpreted together with dynamic elastic parameters, geological information, and verified through soil boring.

3.7 Qualitative Comparison Between Dynamic Elastic Parameters and SPT Data

As the available soil boring location is outside of line 1 and 2, its lithological and SPT data were used only for qualitative comparison. The lithology in Tables 2 and 3 was interpreted from the SRT-derived V_p, with the boring log and N-SPT values used as supporting data. In general, dynamic modulus values increases with depth. This is within the norm of typical soil profile, which is also reflected by the increasing N-SPT values with depth. However, the modulus values derived from SRT is not within the typical range of SPT-derived modulus.

Taking data from 0-2 m depth of line 1, the interpreted Young's modulus from the tests was 50-150 MPa, while the SPT data obtain a value of 4. The interpreted stiffness is the typical range of hard to very hard clay, while in reality obtained from SPT reflects a soft-medium consistency. The same very high interpreted modulus was obtained throughout the measurable depth, both for the Young's modulus and bulk modulus. The shear modulus on the other hand, is in a more sensible range. More detailed description is given in the last column of each table.

The high modulus values are likely due to the strain-dependent nature of soil. Soil under small-strain exhibits large modulus, which quickly decreases with increasing strain (Viggiani & Atkinson, 1995). The interpreted modulus from SRT is likely to be in the small-strain range rather than the stiffness used for engineering design (static stiffness). More studies and comparison with laboratory testings need to be conducted to verify the applicable strain range measured by SRT.

Table 2. Dynamic elastic parameters and interpreted material characteristics along line 1

Depth (m)	Lithology	Dynamic Elastic Parameters of Subsurface Materials	N-SPT Value	Soil Classification	Description
0–2	Soil	G: 20–35 MPa, E: 50–150 MPa, K: 500–2000 MPa, ν: 0.24–0.30 BI: 0.20–0.32	4	Soft–medium boundary	This layer has the lowest Young's modulus along line 1, with its relatively high value attributed to dynamic stiffness, which is generally higher than static stiffness. The nearby N-SPT value of 4 indicates medium consistency.
2–7	Clayey Sand	G: 35–80 MPa, E: 150–200 MPa, K: 2000–4000MPa, ν: 0.35–0.45 BI: 0.04–0.14	5–11	Medium to stiff	The modulus values increase, while the nearby N-SPT values of 5–11 indicate medium-to-stiff consistency
7–15	Clay	G: 80–140 MPa, E: 200–450 MPa, K: 4000–7000 MPa, ν: 0.42–0.48 BI: 0.04–0.34	20	Very stiff	This interval exhibits higher stiffness. The nearby N-SPT value of 20 indicates very stiff consistency
15–20	Clay	G: 140–180 MPa, E: 450–600 MPa, K: 7000–9000MPa, ν: 0.48–0.49 BI: 0.34–0.36	51–60	Hard	The modulus values are relatively high, while the nearby N-SPT values of 51–60 indicate hard soil
15–23	Coal	G: 180–260 MPa, E: 600–800 MPa, K: 7000–10500MPa, ν: 0.48–0.49 BI: 0.36–0.54	> 50	Hard	The possible coal-bearing unit has high modulus and brittleness values. The nearby N-SPT value above 50 indicates hard material

Table 3. Dynamic elastic parameters and interpreted material characteristics along line 2

Depth (m)	Lithology	Dynamic Elastic Parameters of Subsurface Materials	N-SPT Value	Soil Classification	Description
0–1	Soil	G: 20–30 MPa, E: 60–80 MPa, K: 800–1600 MPa, ν: 0.45–0.48 BI: 0.02–0.38	4	Soft–medium boundary	This near-surface layer has the lowest stiffness along Line 2. The calculated dynamic modulus may exceed typical static values, while the nearby N-SPT value of 4 indicates medium consistency.
1–6	Clayey Sand	G: 30–60 MPa, E: 80–200 MPa, K: 1600–4000 MPa, ν: 0.48–0.49 BI: 0.12–0.38	5–11	Medium to stiff	The modulus values increase with depth, while the nearby N-SPT values of 5–11 indicate medium-to-stiff consistency
6–13	Clay	G: 60–110 MPa, E: 200–320 MPa, K: 4000–6000 MPa, ν: 0.48–0.49 BI: 0.12–0.32	20	Very stiff	This interval exhibits moderate-to-high stiffness. The nearby N-SPT value of 20 indicates very stiff consistency
8–18	Coal	G: 80–120 MPa, E: 240–380 MPa, K: 7200–10400MPa, ν: 0.49–0.493 BI: 0.22–0.42	> 50	Hard	The possible coal-bearing unit exhibits relatively high stiffness. The nearby N-SPT value above 50 indicates hard material
13–23	Clay	G: 110–180 MPa, E: 320–540 MPa, K: 6000–7200 MPa, ν: 0.48–0.49 BI: 0.32–0.54	51–60	Hard	The deeper interval exhibits high stiffness, while the nearby N-SPT values of 51–60 indicate hard soil

4 DISCUSSION

The results indicate that shallow subsurface layers along both survey profiles generally exhibit lower elastic parameter values, whereas deeper layers show higher elastic parameter values and relatively higher Poisson's ratios. The increasing values of shear modulus, Young's modulus, and bulk modulus with depth suggest an increase in the dynamic stiffness characteristics of the subsurface materials. This is within the typical norm of soil profile.

The combined distribution of the Poisson's ratio and V_p/V_s ratio show relatively high values in shallow layers, suggesting the possible presence of a saturated zone that may correspond to the groundwater table. This zone is interpreted at depths of approximately 3 m in line 1 and 2.5 m in line 2. Water-saturated zones are commonly characterized by high Poisson's ratio values (≥ 0.45), which correlate with relatively high V_p/V_s ratios (≥ 2.5–3), whereas unsaturated materials generally exhibit lower V_p/V_s ratios (< 1.6) (Uyanik, 2011). In saturated soil and porous geological materials, higher Poisson's ratio values may reflect stronger pore-fluid effects within the material (Lógó et al., 2022). The nearby soil-boring log indicates shallow clayey sand at comparable depths, which is consistent with relatively permeable materials that may facilitate water infiltration. However, because groundwater-level measurements were not reported in the soil-boring log, the interpreted groundwater table cannot be directly verified.

The distribution of the brittleness index reveals variations in subsurface material characteristics. Low brittleness index values (approximately 0.02–0.32) were identified in shallow layers, indicating ductile to less ductile materials, whereas higher values (approximately 0.32–0.54) were observed at depths of approximately 15–23 m along Line 1 and 13–23 m along Line 2, indicating stiffer and more brittle materials. The higher brittleness index values generally correspond to zones with higher elastic modulus values, suggesting that stiffer materials tend to exhibit more brittle behaviour.

The interpreted dynamic elastic parameters were qualitatively compared with nearby standard penetration test (SPT) data. Higher elastic modulus values at depths of 15–23 m along Line 1 and

13–23 m along Line 2 correspond to nearby N-SPT values of 51–60, whereas lower elastic modulus values at shallow depths (0–2 m along Line 1 and 0–1 m along Line 2) correspond to an N-SPT value of 4. However, because the soil-boring location is outside the survey lines, this comparison is considered qualitative rather than a direct point-to-point validation. These results suggest that the integrated SRT and MASW interpretation provides a reasonable representation of the general subsurface layering in the study area.

The shallow subsurface (0–5 m) is characterized by relatively low dynamic elastic parameters, with shear modulus (G) values of 20–35 MPa, Young's modulus (E) values of 50–150 MPa, and bulk modulus (K) values of 500–2,000 MPa along Line 1, and G values of 20–30 MPa, E values of 60–80 MPa, and K values of 800–1,600 MPa along Line 2. These layers are associated with Poisson's ratio (ν) values of 0.24–0.30 and V_p/V_s ratios of 1.7–6.2 along Line 1, and ν values of 0.45–0.48 and V_p/V_s ratios of 2.5–10 along Line 2, indicating relatively low dynamic stiffness and possible pore-fluid influence. The bulk modulus distribution exhibits localized decreases, indicating spatial variations in volumetric stiffness; however, these variations are not consistently observed in the shear modulus and Young's modulus distributions. Therefore, the bulk modulus alone is insufficient to identify a specific weak zone responsible for the observed ground subsidence.

Overall, variations in dynamic elastic parameters, V_p/V_s and Poisson's ratio indicate heterogeneous subsurface conditions that may increase the taxiway's deformation susceptibility. Possible pore-fluid influence in shallow layers may reduce effective stiffness under loading, but the available geophysical and soil-boring data cannot identify the responsible depth or confirm a direct cause of subsidence. The deformation may result from multiple factors, while deeper layers (>15 m) show higher elastic parameters and better mechanical characteristics.

This study has several limitations. Its accuracy depends on the quality and resolution of the previous SRT and MASW datasets. Bulk density was estimated using Gardner's equation, which was developed for sedimentary rocks and may not accurately represent soil-dominated layers, thereby affecting the calculated shear, Young's, and bulk moduli. These are reflected by the abnormally high Young's and bulk moduli when compared to SPT interpreted moduli. Therefore, these values should be treated as apparent small-strain dynamic parameters rather than direct measures of static soil stiffness and cannot independently assess actual stiffness, settlement, or bearing capacity without site-specific laboratory or in-situ calibration.

5 CONCLUSION

This study conducts SRT and MASW measurement to identify the cause of soil subsidence in APT Pranoto Airport. It was revealed that the subsurface materials beneath the taxiway exhibit spatial variations in apparent small-strain dynamic elastic parameters and brittleness index. The shallow depth generally shows lower Young's, shear, and bulk modulus that increases with depth. Deeper intervals generally exhibit higher dynamic modulus and brittleness index values. Relatively high V_p/V_s and Poisson's ratio values were measured in several zones, particularly at depths of approximately 2.5–3 m, which may reflect pore-fluid influence; however, the exact groundwater-table position cannot be directly verified, as it was not reported in the available soil boring log. As the soil boring was conducted outside of the SRT and MASW measurement line, the SPT data provide only a qualitative comparison of the general depth-related layering. It was found that the calculated moduli, especially Young's and bulk moduli, are much higher than moduli obtained from typical SPT correlation. This may be because the stiffness captured by SRT and MASW represent dynamic (small-strain) rather than static soil stiffness (stiffness in engineering level strain). Therefore, these parameters should not be interpreted as direct measures of actual geotechnical soil stiffness. Overall, the results indicate heterogeneous subsurface conditions that may be relevant to the deformation susceptibility of the taxiway. However, the mechanism, cause, and responsible depth interval of the observed ground subsidence cannot be determined from the present data alone. Further investigation using direct deformation monitoring, groundwater observations, and site-specific geotechnical testing is required.

DISCLAIMER

The authors declare no conflict of interest.

AVAILABILITY OF DATA AND MATERIALS

All data are available from the author.

REFERENCES

Abdullah, A., Tamado, P., Setyaningrum, E., Dwi, M. & Fakhri, A., 2019. Bedrock identification using a 2D seismic tomography model on GMSH software and Python in Peyek Mountain Area, Ciseeng, Bogor, West Java. *Lembaran Publikasi Minyak dan Gas Bumi*, 53(3), pp. 151–160.

Alamsyah, A., Lepong, P., Wahidah, W., & Rahmiati, R., 2024. Application of Seismic Refraction Tomography in Determining the Soil Hardness Level in IKN Nusantara Area. *Journal Geocelebes*, 8(1), pp.62-70. https://doi.org/10.20956/geocelebes.v8i1.32159

Altamar, R. P. & Marfurt, K., 2014. Mineralogy-based brittleness prediction from surface seismic data: Application to the Barnett Shale. *Interpretation*, 2(4), pp. T255–T271. https://doi.org/10.1190/INT-2013-0161.1

Fadhli, Z., Anda, S. T., Syukri, M., Karmel, M. E. R., Tutifla, A. S., Hasibuan, P. & Safitri, R., 2022. Ground Surface Quality Assessment Using P-wave Velocity from 2-D Seismic Refraction Method. *Aceh International Journal of Science and Technology*, 11(3), pp.258–265. https://doi.org/10.13170/aijst.11.3.28818

Fatimatuzzahra, R., 2024. *Model stratifikasi dan kekerasan tanah menggunakan metode seismic refraction tomography (SRT) dan standard penetration test (SPT) pada taxiway Bandar Udara APT Pranoto Samarinda.* Samarinda: Skripsi, Universitas Mulawarman.

Gardner, G. H. F., Gardner, L. W. & Gregory, A. R., 1974. Formation velocity and density: The diagnostic basics for stratigraphic traps. *Geophysics*, 39, pp. 770–780. https://doi.org/10.1190/1.1440465

Hamdan, H., Kritikakis, G., Elsamani, M., Harb, M., Abdel-Fattah, M., & Soupios, P., 2025. Enhancing fieldwork productivity in subsurface characterization: advancements in data acquisition with MASW-DS. *Geomechanics and Geophysics for Geo-Energy and Geo-Resources*, 11(1), 1–21. https://doi.org/10.1007/s40948-025-01025-2

Ketelhodt, J. V., Mohamed, K. & Rosli, N. A., 2017. Elastic parameters from compressional and shear wave tomographic survey: A case study from Kuala Lumpur, Malaysia. *Journal of Applied Geophysics*, 140, pp. 79–89. https://doi.org/10.1016/j.jappgeo.2017.03.008

Lógó, B. A. & Vásárhelyi, B., 2022. Theoretical relationship between the confining pressure and Poisson's ratio of intact rock. *Periodica Polytechnica Civil Engineering*, 66(4), pp. 1114–1121. https://doi.org/10.3311/PPci.19208

Mews, K. S., Alhubail, M. M. & Barati, R. G., 2019. A review of brittleness index correlations for unconventional tight and ultra-tight reservoirs. *Geosciences*, 9(9), pp. 319. https://doi.org/10.3390/geosciences9070319

Olafsdottir, E. A., Erlingsson, S. & Bessason, B., 2020. Open-Source MASW Inversion Tool Aimed at Shear Wave Velocity Profiling for Soil Site Explorations. *Geosciences*, 10(8), pp.322. https://doi.org/10.3390/geosciences10080322

Omovie, S. J. & Castagna, J. P., 2020. Relationships between dynamic elastic moduli in shale reservoirs. *Energies*, 13(22), pp. 1–22. https://doi.org/10.3390/en13226001

Rizqulloh, A. & Riyanto, A., 2021. Distribution analysis of brittleness index, Young's modulus, bulk modulus, and Poisson's ratio using the integration of refraction seismic method and MASW: Case study of Fasilkom UI's new building. *Jurnal Geofisika*, 19(2), pp. 12–22. https://doi.org/10.36435/jgf.v19i2.456

Sarkar, R., Kolathayar, S., Drukpa, D., Choki, K., Rai, S., Tshering, S.T. & Yuden, K., 2021. Near-surface seismic refraction tomography and MASW for site characterization in Phuentsholing, Bhutan Himalaya. *SN Applied Sciences*, 3(4), pp. 1–18. https://doi.org/10.1007/s42452-021-04347-4

Simbolon, Z. V., 2023. *Aplikasi multichannel analysis of surface wave (MASW) untuk interpretasi soil stiffness pada taxiway Bandar Udara APT Pranoto Samarinda*. Samarinda: Skripsi, Universitas Mulawarman.

Uyanik, O., 2011. The porosity of saturated shallow sediments from seismic compressional and shear wave velocities. *Journal of Applied Geophysics*, 73, pp. 16–24. https://doi.org/10.1016/j.jappgeo.2010.11.001

Viggiani, G. & Atkinson, J. H., 1995. Stiffness of fine-grained soil at very small strains. *Géotechnique*, 45(2), pp. 249-265. https://doi.org/10.1680/geot.1995.45.2.249

Zawawi, A. F., Sunardi, B. & Prayoedhie, S., 2023. Penentuan klasifikasi tanah dengan menggunakan metode multi-channel analysis of surface waves di Kapanewon Pleret, Kabupaten Bantul. *Jurnal Stasiun Geofisika*, 1(2), pp. 1–5.

- This page is intentionally left blank -